Journal Name

Dynamic Article Links ►

Cite this: DOI: 10.1039/c0xx00000x

www.rsc.org/xxxxxx

ARTICLE TYPE

Gallium fluoroarsenates

Kayleigh L. Marshall,[a] Jennifer A. Armstrong[b] and Mark T. Weller*[a]

Received (in XXX, XXX) Xth XXXXXXXXX 20XX, Accepted Xth XXXXXXXXX 20XX
DOI: 10.1039/b000000x

Six new phases in the gallium-fluoride-arsenate system have been synthesised hydrofluorothermally using a fluoride-rich medium and "$HAsF_6$" ($HF:AsF_5$) as a reactant. $RbGaF_3(H_2AsO_4)$, $KGaF(H_2AsO_4)$ and [piperazine-H_2]$_2$[$Ga_2F_8(HAsO_4)$]·H_2O have one dimensional structures, [DABCO-H_2]$_2$[$Ga_4F_7O_2H(AsO_4)_2$]·$4H_2O$ consists of two dimensionally connected polyhedral layers, while $GaF(AsO_3[OH,F])_2$ and $(NH_4)_3Ga_4F_9(AsO_4)_2$ both have three-dimensionally connected polyhedral frameworks.

Introduction

Materials adopting structures formed by linking metal centres through tetrahedral oxopolyhedra, such as PO_4, AlO_4, SiO_4, AsO_4 and SO_4, are of considerable interest due to their actual, and potential, applications. These uses include Li-ion battery cathodes [1], applications in a wide range of catalysis processes (including oxidative dehydration catalysts[2]), magnetic materials[3] and pigments[4]. Some clays and the related layered double hydroxides (LDHs) show similar structural motifs with their layers formed from linked tetrahedra and octahedra. Additional applications of this group of materials include ion-exchange, adsorption, and potentially as drug delivery agents. Functionality in many of these applications arises from the combination of a rigid and stable structure formed from linked polyhedra with accessible interlayer spaces or pores, as exemplified by the porous aluminosilicate zeolites[5], related aluminophosphates and the LDHs[6].

Structures based on metal centres connected through oxygen may also be used as precursors for other functional materials following a further chemical reaction that can preserve all or some structural elements or crystal morphology of the original structure. Thus extra-framework template molecules are readily removed from zeolites on mild heating, while at higher temperatures partial removal of framework oxygen atoms generates catalytically-active Lewis acid forms. The partial chemical reduction of metal oxides can result in lower metal oxidation state derivatives following extraction of oxide; for example the formation of $Sr_3Fe_2O_6$ from $Sr_3Fe_2O_7$ and $SrFeO_2$ from $SrFeO_3$.[7, 8] Under more vigorous reaction conditions, e.g. high temperatures it becomes possible to remove the oxygen completely but leave metal or metalloid scaffolding that retains the original porous structural features; of specific note here is the generation of three-dimensional microporous silicon from silica micro-assemblies[9]. The properties of these structured semiconductors, such as photoluminescence, offer potential applications in sensors, electronic and biomedical applications. The ability to structure silica into many forms, including the siliceous zeolites and the natural microshells, is well known but for other important semiconductor materials, e.g. GaAs, CdTe, there are currently very few suitable precursor compounds. Therefore routes to making framework structures with compositions that reflect those of functional semiconductor after reduction are of some significance.

Considerable effort has been directed at the synthesis and characterisation of gallophosphate materials mainly as the "$GaPO_4$" building unit is isostructural and isoelectronic with the $AlPO_4$ and SiO_2 and, thereby, forms fully connected, three-dimensional framework structures of interest in catalysis and molecular separations. One gallophosphate framework of considerable note is the –**CLO** structure of $|(C_7H_{14}N^+)_{24}|_8$ $[F_{24}Ga_{96}P_{96}O_{372}(OH)_{24}]_8$ which has a 20-T atom pore.[10] This structure is not full three dimensionally connected but contains terminal OH and F groups. Approximately 20 gallosilicate and 10 gallophosphate zeotype structures are known, including those adopting the framework codes **CGS**, **CZP**, **UEI** and **RHO**. Structures containing gallium in combination with arsenate as oxotetrahedral units are much rarer and examples of zeotype frameworks formed partially from galloarsenate units are limited to those also incorporating zinc, that is [Zn-Ga-As-O]-GIS[10], Zn-Ga-As-O]-SOD[11] and [Zn-Ga-As-O]-KFI.[12]

In general the products of reactions using gallium and arsenate in hydrothermal media lie on the borderline between those adopting structures with six coordinate octahedral gallium and those, such as the zeotypes, with GaO_4 units. Normally these gallium centred polyhedra occur in combination with tetrahedral arsenate(V) or hydrogenarsenate(V), though octahedral arsenate(V) can also form.[12-15] Examples of structures formed from octahedral gallium in combination with arsenate include the high pressure phase *P*3-$GaAsO_4$.[16]

We have recently reported that further compositional, and, therefore, structural, variability beyond oxopolyhedral units in materials can be achieved by the introduction of additional

anionic species, such as a halide (X^-, X = F, Cl), into a material. The addition of F^- into a solvothermal reaction mixture at low concentrations generally acts as a mineralising agent,[17] while at higher molar concentrations in the reaction medium it is often incorporated into the products. Examples of materials combining both oxo-tetrahedra and high levels of fluoride anions in a framework material are still comparatively rare, though reported examples include fluoro-vanadyl-hydrogenarsenates[18] and cerium fluoroarsenate frameworks.[19] A summary of the use of fluoride-rich hydrothermal media to synthesise mid- to late- first row transition metal fluorophosphates has been published.[21] Since then we have extended considerably the range of metal fluorophosphates synthesised and characterised.[20-24] Here we describe the results of work carried out on gallium fluoroarsenate materials. Trends in compositional and structural features for these Ga-based materials are analysed and discussed.

Experimental

Synthesis.

All samples were prepared from, at the time, commercially available materials of reagent grade that did not require further purification, with the exception of GaO(OH), which was obtained by the hydrothermal treatment of gallium metal dissolved in *aqua regia,* concentrated HCl/HNO_3 (aq). Note that while a reagent of composition "$HAsF_6$" used to be sold by Apollo Scientific it is no longer available and the existence of a compound with this stoichiometry has recently been called into doubt.[25] Formally "$HAsF_6$" may be obtained by dissolving AsF_5 in HF and this provides an alternative route to these materials. **Warning!** Caution should be taken due to the potentially violent nature of the reactions, with generation of HF gas (very toxic by inhalation, in contact with skin and if swallowed) as a side product. All the compounds were synthesised hydrothermally on a mmol scale and reactions were performed in a 23mL Teflon™-lined Parr autoclave; reaction conditions, compositions and yields are summarised under each phase description. Products were collected by filtration, washed with distilled water and dried in air at 80 °C overnight.

X-ray diffraction studies

Single-crystal X-ray diffraction (SXD) data were collected at 120 K on a Bruker Nonius Apex II CCD diffractometer, using Mo-Kα (λ=0.71073 Å) radiation for structures I-III and at 150 K on an Agilent Supernova, dual tube Eos S2 CCD diffractometer operating Cu-Kα (λ=1.54178 Å) radiation for structures IV-VI. Structures were solved using the WinGX suite of programmes,[26] utilising XPREP[27] and SHELX-97,[28] by direct methods.[29] All non-hydrogen atomic displacement parameters were refined anisotropically, using the F^2 least-squares method. Details of all the single crystal refinements are summarised in Table 1. Assignment of sites as oxygen or fluorine was undertaken using a combination of data fitting, charge balancing and bond valence calculations. In general, initial allocation of an oxide ion to an anion site yielded non-positive or very small ADP values if this site was fluoride; reassignment of this scattering power as fluoride produced similar ADP values for all anion sites. Where such analysis was ambiguous charge balance considerations were employed in combination with anion site bond valence calculations, which readily distinguish sites with −1 and −2 charges. For example, in such calculations incorrect assignment of an oxide ion to a fluoride ion site (during structure refinement) produced low values for the site valence, <1.3, indicative of a fluoride ion at this position; in such cases the crystallographic model was updated appropriately. In a few products the potential for the presence, including partially, of hydroxide instead of fluoride existed and the dominance of heavy atom scattering meant it was impossible to locate hydrogen atoms in a possible hydroxide group. In these cases the product formula is represented as a mixture of OH and F, i.e. (OH,F).

Structure	Formula weight	Crystal System	Space group	Unit cell dimensions (Å/°)	Volume (Å^3)	*Z*	*R* indices all data	*R* indices observed data	GOOF
I $GaF(AsO_2[OH,F]_2)_2$	366.6	Tetragonal	*I*4/*mcm*	*a*, *b* = 9.076(4) *c* = 7.860(6)	647.46(1)	4	R_1= 0.055 wR_2= 0.097	R_1= 0.046 wR_2= 0.094	1.153
II $KGaF_3(H_2AsO_4)$	304.7	Monoclinic	*P*2/*n*	*a* = 7.1901(2) *b* = 7.7981(2) *c* = 10.9297(4) *β* = 102.245(2)	598.88(3)	4	R_1 = 0.038 wR_1 = 0.095	R_1 = 0.033 wR_1 = 0.091	1.180
III $RbGaF_3(H_2AsO_4)$	353.1	Monoclinic	*C*2/*c*	*a* = 11.8591(10) *b* = 8.6109(8) *c* = 7.2500(6) *β* = 120.616(5)	637.15(22)	4	R_1 = 0.059 wR_1 = 0.087	R_1 = 0.044 wR_1 = 0.081	1.148
IV $(NH_4)_3Ga_4F_9(AsO_4)_2$	769.7	Monoclinic	*P*2/*m*	*a* = 7.1120(3) *b* = 14.4865(6) *c* = 7.5563(4) *β* = 106.751(5)	745.48(12)	2	R_1= 0.050 wR_2= 0.129	R_1= 0.046 wR_2= 0.124	1.026
V [Piperazine-$H_2]_2[Ga_2F_8(HAsO4)]\cdot H_2O$	638.4	Orthorhombic	*Pbca*	*a* = 12.9563(2) *b* = 13.6686(2) *c* = 41.1833(5)	7293.33(2)	16	R_1=0.060 wR_2=0.145	R_1= 0.053 wR_2= 0.138	1.017
VI [DABCO-$H_2]_2[Ga_4F_7O_2H(AsO_4)_2]\cdot 4H_2O$	1014.1	Orthorhombic	$P2_12_12$	*a* = 10.3300(3) *b* = 10.3820(4) *c* = 12.3413(5)	1323.59(1)	2	R_1= 0.056 wR_2= 0.143	R_1= 0.054 wR_2= 0.140	1.076

Table 1 Summary of the crystallographic information for all compounds

Results and Discussion

Compound **I GaF(AsO$_2$[OH,F]$_2$)$_2$**

GaF(AsO$_2$[OH,F]$_2$)$_2$ was obtained from the reaction of GaOOH, HAsF$_6$ and LiF in stoichiometric amounts heated at 180 °C for 72 hours; the product was isolated as colourless blocks in an estimated 50 % phase purity; GaAsO$_4$ was identified as the major impurity phase from PXD data, see ESI. GaF(AsO$_2$[OH,F]$_2$)$_2$ crystallises with a tetragonal unit cell and a highly regular arrangement of GaF$_2$O$_4$ octahedra and AsO$_2$[OH,F]$_2$ tetrahedra. The GaF$_2$O$_4$ octahedra have trans-fluoride ions which are shared between gallium centres along the *c*-axis direction to produce infinite chains. Adjacent chains are arranged in a regular square array with respect to a central chain and the columns displaced by *c*/2, Figure 1. Adjacent chains are cross-linked by four fluoro-/hydroxyl-arsenate tetrahedra connected at each of the four meridinal GaF$_2$O$_4$ octahedron oxygen atoms and connected alternately up-down with respect to their directionality around each gallium centre and to its nearest neighbour chain. This produces narrow channels which also run along the *c*-axis direction. The potential exists for a hydrogen bond between adjacent terminal anions on the arsenic centres with the (OH,F)….(OH,F) distance at 2.7694(79) Å and a possible scenario is that locally pairs of OH…F units occur.

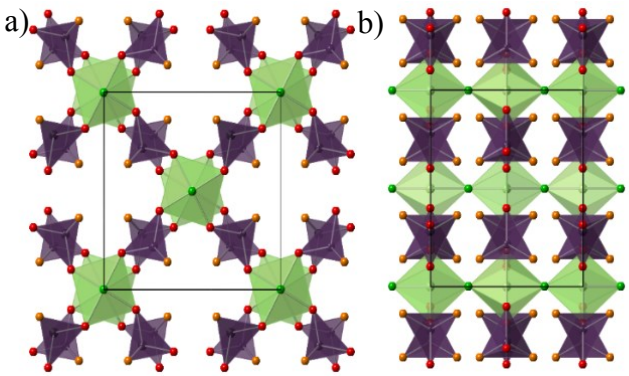

Figure 1 Crystal structure of GaF(AsO$_3$[OH,F])$_2$ viewed along the *c*-axis (a) and *b*-axis (b). Colour key: GaO$_4$F$_2$ octahedra in pale green, AsO$_3$[OH,F] tetrahedra in dark purple, oxygen and fluorine atoms in red and green respectively, with the mixed OH/F sites in orange. The unit cell is outlined.

Compound **II KGaF$_3$(H$_2$AsO$_4$)**

KGaF$_3$(H$_2$AsO$_4$) was obtained from the reaction of GaOOH, HAsF$_6$ and KF in stoichiometric amounts heated at 180 °C for 72 hours; the product was isolated as colourless blocks in an estimated 70% phase purity. KGaF$_3$(H$_2$AsO$_4$) crystallises with a monoclinic unit cell and consists of zig-zag chains of interconnected GaF$_4$O$_2$ octahedra and H$_2$AsO$_4$ tetrahedra with potassium ions in the interchain space (Figure 2). The gallium centres are connected via bridging fluoride ions and hydrogenarsenate tetrahedra as shown in Figure 3. The two distinct gallium sites alternate along the chains which run diagonally in the *ac* plane and are stacked directly above each other in the *a* and *b* directions. For Ga1 two *cis*-fluoride ions bridge to two neighbouring Ga2 centres while the other two fluoride ions are oriented towards the OH groups of arsenate

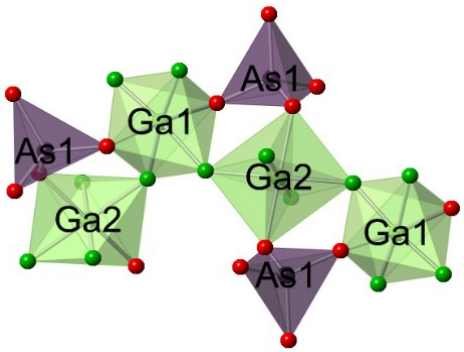

Figure 2 Connectivity of zig-zag chains in KGaF$_3$(H$_2$AsO$_4$). Colour key: GaF$_4$O$_2$ octahedra in pale green, AsO$_4$ tetrahedra in dark purple, oxygen and fluorine atoms in red and green respectively

tetrahedra on adjacent chains forming hydrogen bonds with O-H…F distances of 2.5865(41) Å. The terminal fluoride ions on Ga2 adopt a *trans* configuration and are also oriented towards OH groups forming hydrogen bonds with O-H…F distances of 2.5210(42) Å. The K+ ions have 10 surrounding O/F anions at distances between 2.7000(28) and 3.6149(33) Å.

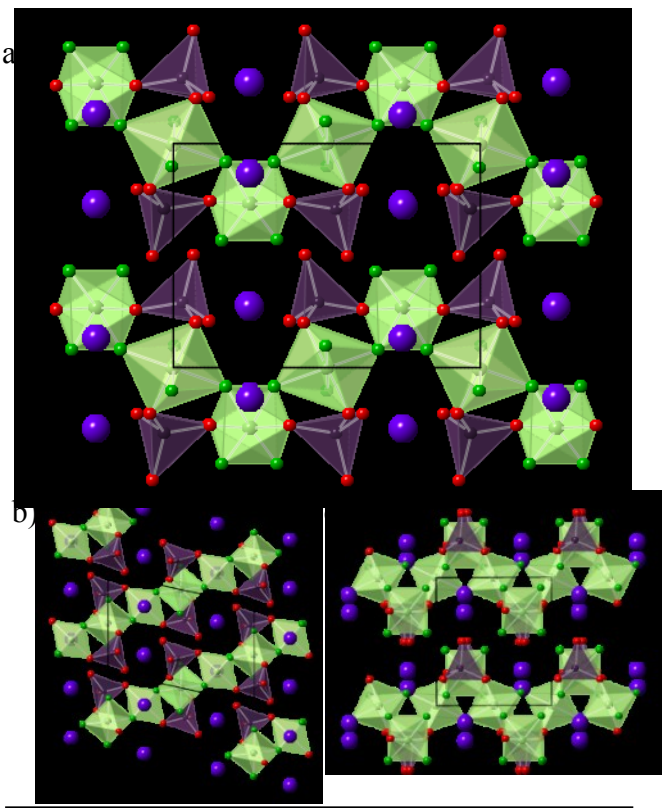

Figure 3 Crystal structure of KGaF$_3$(H$_2$AsO$_4$) viewed along the *a*, *b*- and *c*-axes (a), (b) and (c) respectively. Colour key: GaF$_4$O$_2$ octahedra in pale green, AsO$_4$ tetrahedra in dark purple, oxygen and fluorine atoms in red and green respectively, and potassium cations in purple. The unit cell is outlined.

Compound **III $RbGaF_3(H_2AsO_4)$**

$RbGaF_3(H_2AsO_4)$ was obtained from the reaction of GaOOH, $HAsF_6$ and RbF in stoichiometric amounts heated at 180 °C for 72 hours; the product was isolated as colourless blocks in an estimated 80% phase purity. $RbGaF_3(H_2AsO_4)$ also crystallises with a monoclinic unit cell but consists of linear chains of inter connected GaF_4O_2 octahedra and H_2AsO_4 tetrahedra with rubidium ions in the interchain space (Figure 4). Each gallium centre is connected to the next in the chain via a bridging fluoride anion and dihydrogeno-arsenate tetrahedra bridging the two *trans*-oxide anions. The terminal *trans*-fluoride ions coordinated to the gallium centres are oriented towards terminal OH groups on arsenate tetrahedra from adjacent chains forming hydrogen bonds with O-H…F distances of 2.5884(65) Å. This results in the alternating stacking of the chains in the *a* cell direction (Figure 4a) and the offset in the *c* direction (Figure 4c). The rubidium ions are surrounded by six fluoride and four oxygen atoms of hydroxide anions at distances between 2.8499(51) and 2.9554(42) Å and with a nearest rubidium ion neighbour distance of 5.628(180) Å.

Compound **IV $(NH_4)_3Ga_4F_9(AsO_4)_2$**

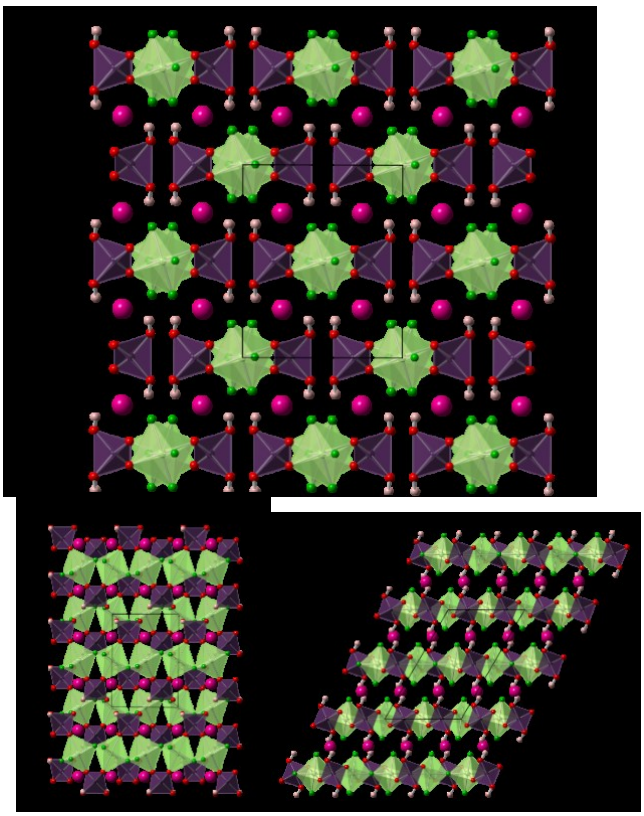

Figure 4 Crystal structure of $RbGaF_3(H_2AsO_4)$ viewed along the *c*-axis (a), *a*-axis (b) and *b*-axis (c). Colour key: GaF_4O_2 octahedra in pale green, AsO_4 tetrahedra in dark purple, oxygen and fluorine atoms in red and green respectively, and rubidium cations in dark pink. The unit cell is outlined.

$(NH_4)_3Ga_4F_9(AsO_4)_2$ was obtained from the reaction of GaOOH, $HAsF_6$ and NH_4F in stoichiometric amounts heated at 180 °C for 72 hours; the product was isolated as colourless rectangular blocks in a 100% phase purity. $(NH_4)_3Ga_4F_9(AsO_4)_2$ is isostructural

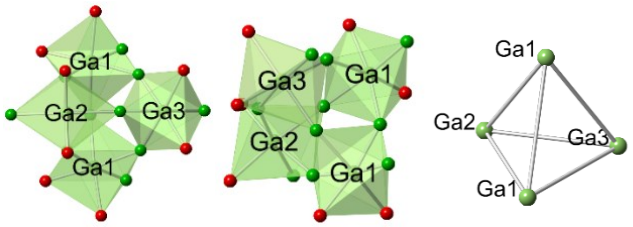

Figure 5 Connectivity of gallium centres in $(NH_4)_3Ga_4F_9(AsO_4)_2$. From left to right: view down the *c*-axis, slightly off set view down the *a*-axis and oxygen and fluorine atoms removed to show tetrahedral arrangement on Ga centres. The unit cell is outlined.

$(NH_4)_3Fe_4F_9(PO_4)_2$,[21] and crystallises with a monoclinic unit cell consisting of a 3D network of interconnected GaF_4O_2 octahedra and AsO_4 tetrahedra with ammonium cations occupying in the pore centres. There are three distinct gallium centres within the 3D framework, which connect together in groups of four (2 x Ga1, 1 each x Ga2 and Ga3) interconnected via bridging fluoride ions in a tetrahedral arrangement (Figure 5); these "tetrahedra-of-octahedra" units are connected via a bridging fluoride ion to produce chains along the *a*-axis. Further bridging though oxygen atoms to AsO_4 tetrahedra along and between these chains produces the complete 3D framework, Figure 6.

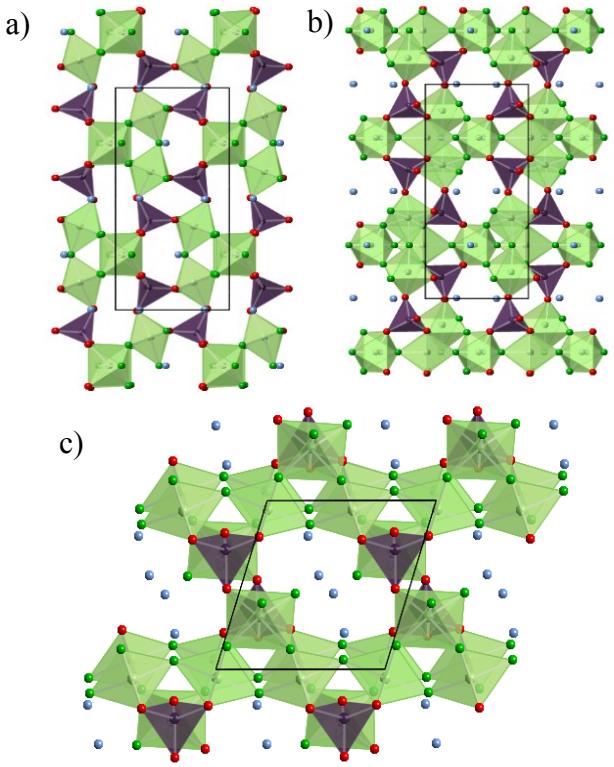

Figure 6 Crystal structure of $(NH_4)_3Ga_4F_9(AsO_4)_2$ viewed along the *a*-axis (a), *c*-axis (b) and *b*-axis (c). Colour key: GaF_4O_2 octahedra in pale green, AsO_4 tetrahedra in dark purple, oxygen and fluorine atoms in red and green respectively, and nitrogen atoms in pale blue. The unit cell is outlined.

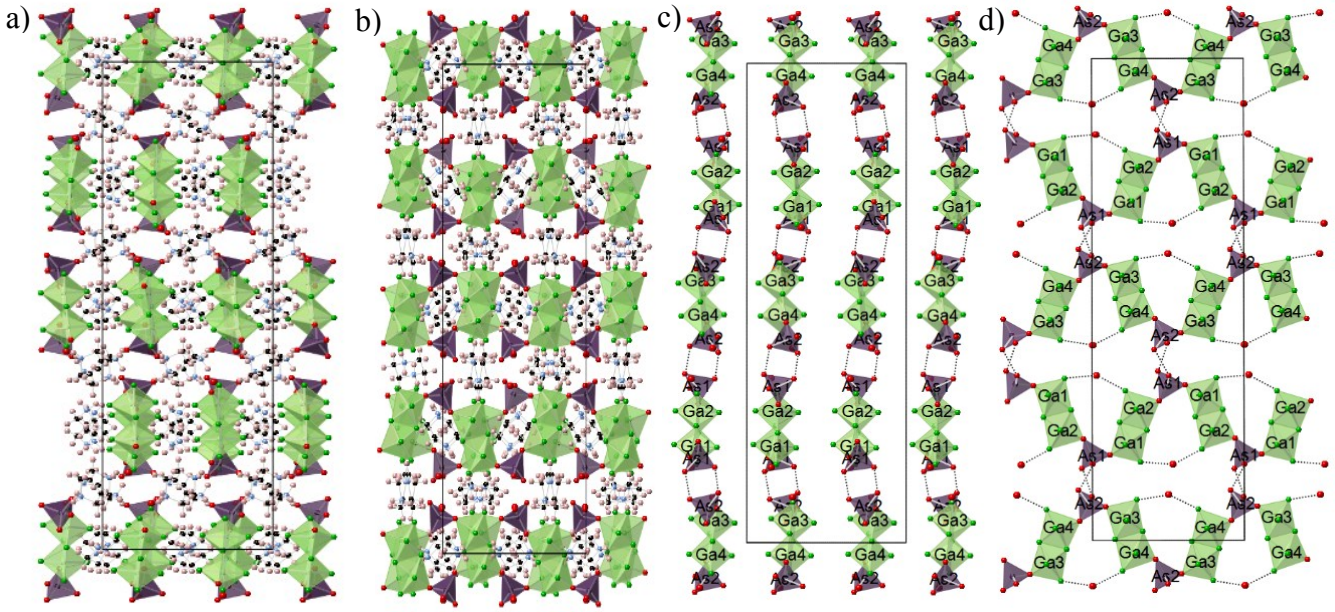

Figure 7 Crystal structure of [piperazine-H_2]$_2$[$Ga_2F_8(HAsO_4)$]·H_2O viewed down the *a*- and *b*- axes; (a) and (b) respectively and (c) and (d) showing the hydrogen bonding between $HAsO_4$ groups and the structure directing water molecules and terminal fluorides down the *a*- and *b*- axes respectively Colour key: GaF_5O octahedra in pale green, $HAsO_4$ tetrahedra in dark purple, oxygen and fluorine atoms in red and green respectively, and carbon, nitrogen and hydrogen atoms in black, pale blue and pale pink respectively. The larger red spheres represent oxygen atoms of the water molecules and the dashed black lines show the hydrogen bonds. The unit cell is outlined.

The remaining terminal fluoride ion within the structure, coordinated to Ga1, is oriented into the channels, which run parallel to the *b*-axis, giving them a distorted figure of eight shape (similar to that seen previously with two titanium fluorophosphate structures[30]). Towards the edges of the 'lobes' of the channels reside the ammonium cations at N-H…F/O distances between 2.7897(59) and 2.9864(77) Å.

Compound **V [Piperazine-H_2]$_2$[$Ga_2F_8(HAsO_4)$]·H_2O**

[Piperazine-H_2]$_2$[$Ga_2F_8(HAsO_4)$]·H_2O was obtained from the reaction of GaOOH, $HAsF_6$ and piperazine in stoichiometric amounts heated at 180 °C for 72 hours; the product was isolated as colourless blocks with a slight yellow tinge in an estimated 60% phase purity. [Piperazine-H_2]$_2$[$Ga_2F_8(HAsO_4)$]·H_2O crystallises with an orthorhombic unit cell consisting of zig-zag chains of interconnected GaF_5O octahedra and $HAsO_4$ tetrahedra with structure directing water molecules and doubly protonated piperazine molecular cations in the inter-chain space, Figure 7. There are four distinct Ga-sites and two distinct As-sites within the structure which generate two unique chain-type features which alternate along the *c* direction. Both chains comprise of pairs of edge sharing (via two fluoride ions) GaF_5O octahedra which are connected to the adjacent $[Ga_2F_8O_2]$ doublet in the *a* direction via a vertex sharing of $HAsO_4$ tetrahedra, Figure 7d. On adjacent chains in the *c* direction, the terminal oxygens on the $HAsO_4$ are tilted towards each other such that two hydrogen bonds are formed at distances of 2.5597(57) and 2.5674(56) Å (Figure 7c) giving "layers" of alternating hydrogen bonded chains in the *ac* plane. Terminal fluoride ions adjacent to the $HAsO_4$ groups within the chains are also hydrogen bonded to the interchain water molecules, with F...H-O distances between 2.7706(75) and 2.9613(90) Å (Figure 7d). The "layers" of hydrogen bonded chains are stacked in the *b* direction such that the $HAsO_4$ groups lie adjacent to the water molecule in the next "layer" (alternating stacking arrangement).Between the "layers" there are four distinct doubly protonated piperazine molecular cations which participate in moderate to strong inter-chain hydrogen bonding with terminal fluorides, (hydr-)oxides and the water molecules at N-H…O/F distances between 2.5741(53) and 3.0166(60) Å. It is the orientation of these molecular cations along with the alternating chains within the hydrogen bonded "layers" within this structure that result in the long *c*-axis of 41.1833(5) Å.

Compound **VI [DABCO-H_2]$_2$[$Ga_4F_7O_2H(AsO_4)_2$]·$4H_2O$**

[DABCO-H_2]$_2$[$Ga_4F_7O_2H(AsO_4)_2$]·$4H_2O$ was obtained from the reaction of GaOOH, $HAsF_6$ and DABCO in stoichiometric amounts heated at 180 °C for 72 hours; the product was isolated as colourless blocks with a slight yellow tinge in an estimated 65% phase purity. [DABCO-H_2]$_2$[$Ga_4F_7O_2H(AsO_4)_2$]·$4H_2O$ crystallises with an orthorhombic unit cell consisting of net-like sheets of interconnected GaF_3O_3 octahedra and AsO_4 tetrahedra with doubly protonated DABCO molecular cations and structure directing water molecules in the inter-layer space (Figure 8). There are two distinct gallium centres within this structure which are connected directly to one another via two bridging fluoride anions, with each pair of gallium centres being connected to one another by a bridging fluoride and two arsenate tetrahedra to give the secondary building unit highlighted in figure 8c. These building units connect though the Ga1-O-As1-O-Ga2 bridges in

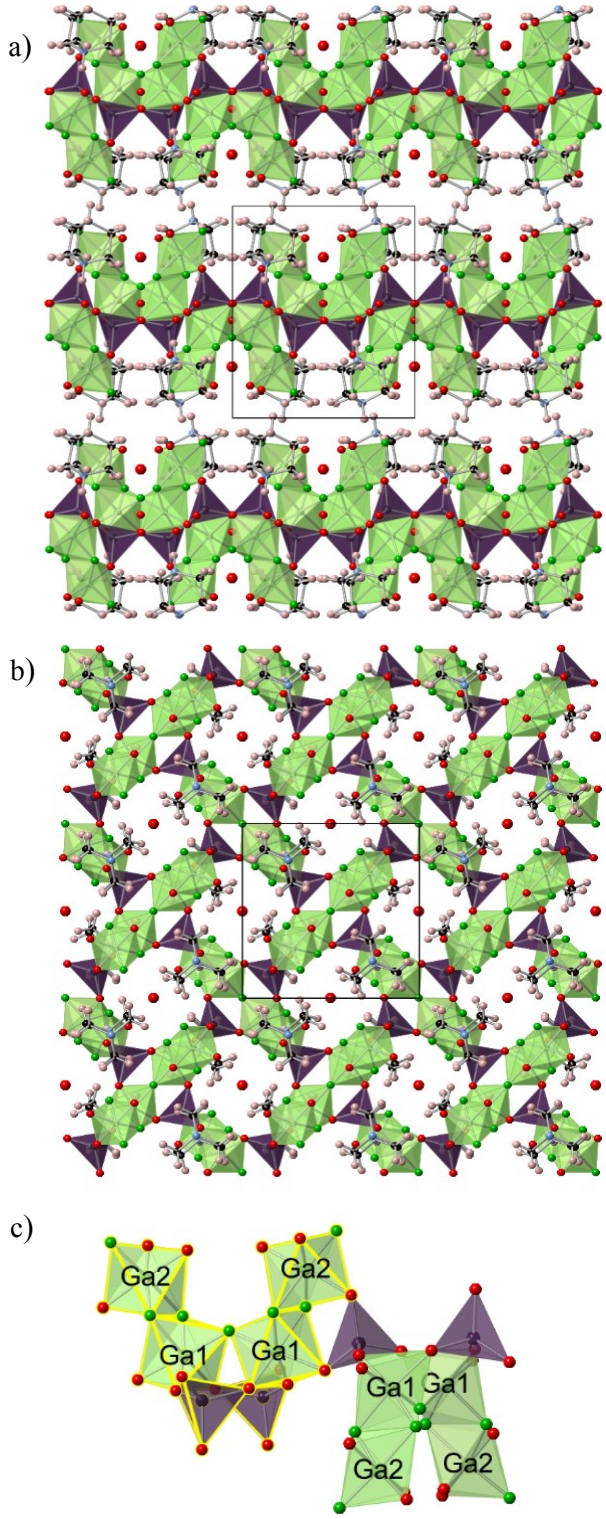

Figure 8 Crystal structure of [DABCO-H_2]$_2$[$Ga_4F_7O_2H(AsO_4)_2$]·$4H_2O$ viewed down the *a*-axis and *c*-axis (a) and (b) respectively. (c) shows two secondary building units and the two distinct gallium centres, one is highlighted in yellow Colour key: GaF_4O_2 octahedra in pale green, AsO_4 tetrahedra in dark purple, oxygen and fluorine atoms in red and green respectively, and carbon, nitrogen and hydrogen atoms in black, pale blue and pale pink respectively. The larger red spheres represent oxygen atoms of the water molecules. The unit cell is outlined

an alternating arrangement, giving the net-like layers with the Ga2 octahedra lining the edges. There are two terminal oxygen atoms attached to the Ga2 centres, one forms hydrogen bonds with a structure directing water molecule while the other forms a moderately strongly hydrogen bonded O-H….O unit whereby a proton randomly occupies a site between the two symmetry related oxygen atoms which lie only 3.0452(54) Å apart. There is also a terminal fluoride ion on Ga2 which is oriented towards the inter-chain space and has the possibility of forming hydrogen bonds with the doubly protonated DABCO molecular cations with F…H distances between 2.1887(65) and 2.5024(49) Å. The layers stack directly above one another in the *c*-direction so that there are channels running perpendicular to the layers, in which the two water molecules sit hydrogen bonding with each other and terminal ions on gallium-centred octahedra.

Thermal decomposition and reduction of gallium fluoroarsenates; see ESI for details.

Samples of **I**, **IV**, **V** and **VI** were investigated by thermogravimetric analysis (TGA) under nitrogen gas between room temperature and 700 °C. Separately, reductions of Compounds **I**, **IV**, **V** and **VI**, were carried out in a sealed tube furnace under a flowing 10% H_2/N_2 gas mix at various temperatures, *vide infra*, for between 1 and 1.5 hours. The sample of Compound **I** (which is ~50% $GaF(AsO_2[OH,F]_2)_2$ and 50% $GaAsO_4$ visually and from PXD) proved to be thermally stable to 275 °C before a rapid weight loss of approximately 4.6 %. Reduction of Compound **I** under flowing H_2/N_2 gas at 150 °C for 1 hour produced a white crystalline solid mixture containing a higher proportion of $GaAsO_4$, as identified from PXRD. The weight loss of 4.6% is consistent with loss of water from a 50% pure sample of $GaF(AsO_2[OH,F]_2)_2$ of composition $GaF(AsO_2(OH)F)_2$ (calculated weight loss 4.91%). Compound **IV** proved relatively thermally stable up to 300 °C, at which point a loss of approximately 7% mass occurred up to 450 °C. This weight loss can be attributed to the loss of NH_3 from within the framework and formation of $H_3Ga_4F_9(AsO_4)_2$ (calculated weight loss 6.6%). Two subsequent steep weight losses, each of around 15% and occurring between 450-530 °C and 550-650 °C correspond to further decomposition, framework destruction, and loss of H_2O and, presumably, HF (CARE – see experimental). Reductions of Compound **IV** under flowing H_2/N_2, at 530 °C for 1.5 hours and 700 °C for 1 hour, both produced a brown amorphous powder (from PXRD data). Thermogravimetric traces for Compounds **V** and **VI** both showed very gradual thermal decomposition with approximately 60% weight losses from 50 -700 °C, consistent with the initial decomposition of the organic template at lower temperatures and likely framework decomposition/reduction and H_2O/HF evolution at higher temperatures. Reduction of both these compounds under flowing H_2/N_2 at 500 °C produced finely divided black powders identified as cubic phase GaAs by PXRD.

Conclusions

Six new gallium fluoro-hydroxyarsenate structures have been synthesised, *via* fluoride-rich hydrothermal methods, and characterised by SXD. The structures produced exhibit a number of new and previously seen, in metal fluoro-oxotetrahedra materials, structural features. These are derived from combined structure directing effects of the fluoride anions and oxo-

tetrahedral species, As(V)$(O,OH)_4$, coupled to the size and coordination preferences, including hydrogen bonding, of templating cations.

In the compounds described in this article the fluoride ion is almost only found bonded to gallium, rather than forming $T(O_{4-n}F_n)$ tetrahedral units as are found reasonably frequently with phosphorus in metal fluorophosphates.[21] While arsenic(V) forms six-fold coordination in some structures, and particularly in combination with fluoride, e.g. the $[AsF_6]^-$ anion, under the conditions used in this study arsenic was only found in tetrahedral coordination to oxygen. The fluoride ions on arsenic form a mixture of bridging, to other gallium centres, and terminal sites with bridging positions being more common as found in Compound **I** (bridging only), Compound **II** (1 bridging, 2 terminal), Compound **III** (1 bridging, 2 terminal), Compound **IV** ((5 bridging, 1 terminal), Compound **V** ((2 bridging, 6 terminal) and Compound **VI** (3 bridging, 1 terminal). This preference for bridging positions on a 3+ cation mirrors that found previously for iron; this contrasts with the behaviours with lower charged metal centres where terminal fluoride ion positions are more prevalent.[21] This variation in bridging versus terminal fluoride ion content coupled with the overall gallium to fluorine ratio may be used to explain the dimensionality of the structures found; compounds **II**, **III**, and **V** are one dimensional formed of single metal chains or ribbons, while **VI** has a two dimensional layered structure and **I** and **IV** are three-dimensional structures. The fluorine to gallium ratios for the six compounds are 1, 3, 3, 2.25, 4 and 1.75 respectively and the terminal fluoride ion to bridging fluorine ion ratios are 0, 2, 2, $^1/_5$, 3, and $^1/_3$. Thus high levels bridging fluoride ions lead to framework structures while high levels of terminal fluoride ions disrupt the connectivity giving one-dimensional structures. Higher overall levels of fluoride in relation to that of gallium also have a tendency to disrupt connectivity.

The polyhedral connectivity of structures **III** and **IV** have been observed previously for other metal fluorophosphate and fluorosulfate compounds,[21,23] with the simple chain of **III** being very common - though the distribution and separation of the parallel chains varies enormously depending on the nature and the size of the cation. Of note is the different chain formed in Compound **III** in comparison with that found in **II,** especially given that the these materials have equivalent compositions, $AGaF_3(H_2AsO_4)$, A = K, Rb, but just slightly different sized cations, $r(Rb^+) = 1.49$Å and $r(K^+) = 1.38$ Å. In $RbGaF_3(H_2AsO_4)$ chains are formed from a single type of GaO_2F_4 octahedron sharing *trans* fluoride ions while in $KGaF_3(H_2AsO_4)$ one type of GaO_2F_4 octahedron shares *trans* fluoride ions while the second shares *cis* fluoride ions. This causes the polyhedral chains to become notably zig-zag and allows strong coordination to the smaller potassium ion sitting in the alternate up-down pockets of the zig-zag chain.

Use of organic templating cations as in Compounds **V** and **VI** leads to crystallographically much more complex structures as the directional hydrogen bonding interactions between the cations and polyhedral units becomes a significant driving force in the arrangement of these structural units.

This work has shown that the formation of gallium arsenate framework structures can be achieved under hydrofluorothermal conditions and six new materials from this family have been described.

Given the ability to reduce similar SiO_2 frameworks to semiconductor structures[9] initial thermal studies have been carried out on compounds **I**, **IV**, **V** and **VI**. For the inorganic compounds **I** and **IV** decomposition in nitrogen or 10% H_2/N_2 results in loss of water/HF/ammonia though even under reducing conditions Compound **I** is not reduced from As(V). However, with organic templating species, as in Compounds **V** and **VI,** reaction under reducing conditions at 500 °C results in the formation of impure, cubic GaAs. This greater level of reduction may reflect a role for the organic template in the reductive decomposition process.

The ability to produce GaAs from a framework oxide-fluoride under reasonably mild conditions, 10% H_2/N_2 at 500°C contrasts strongly with those necessary for the reduction of SiO_2 to Si. Such conditions are similar to those typically used for the Chemical Vapour Deposition of GaAs from Me_3Ga/AsH_3 (600-700°C) or single source precursors.[31] While the GaAs formed under these conditions is finely divided, impure (reflecting the non 1:1 Ga:As ratios of compounds **V** and **VI)** and does not retain the crystal morphology of framework precursor the results of work demonstrate the potential for a new route to depositing GaAs-precursor materials.

Acknowledgements

The authors would like to thank the University of Bath for studentship funding for KLM.

Notes and references

[a] * *Department of Chemistry, University of Bath, Bath BA2 7AY. E-mail m.t.weller@bath.ac.uk. Tel:+44 (0) 1225 386531*
[b] *School of Chemistry, University of Southampton, Highfield Campus, Southampton, Hampshire, SO17 1BJ, UK.*

References

1. A. K. Padhi, K. S. Nanjundaswamy and J. B. Goodenough, *J. Electrochem. Soc.*, 1997, 144, 1188-1194.
2. P. Bonnet, J.-M. M. Millet, C. Leclercq and J. C. Vedrine, *J. Catal.*, 1996, 158, 128-141.
3. M. Riou-Cavellec;, D. Riou; and G. Ferey;, *Inorg. Chim. Acta*, 1999, 291, 317-325.
4. G. Buxbaum and G. Pfaff, *Industrial Inorganic Pigments*, Wiley-VCH, Morlenbach, 2005.
5. S. T. Wilson, B. M. Lok, C. A. Messina, T. R. Cannan and E. M. Flanigen, *J. Am. Chem. Soc.*, 1982, 104, 1146-1147.
6. S. E. Dann and M. T. Weller, *J. Solid State Chem.,* 1995, 115, 499-507.
7. D. Walsh, L. Arcelli, T. Ikoma, J. Tanaka and S. Mann, *Nature Materials*, 2003, 2, 386-U385.
8. M. Estermann, L. B. McCusker, C. Baerlocher, A. Merrouche and H. Kessler, *Nature*, 1991, 352, 320-323.
9. Z. Bao, M. R. Weatherspoon, S. Shian, Y. Cai, P. D. Graham, S. M. Allan, G. Ahmad, M. B. Dickerson, B. C. Church, Z. Kang, H. W. Abernathy Iii, C. J. Summers, M. Liu and K. H. Sandhage, *Nature*, 2007, 446, 172-175.
10. P. Feng, T. Zhang and X. Bu, *J. Amer. Chem. Soc.*, 2001, 123, 8608-8609.
11. X. Bu, T. E. Gier, P. Feng and G. D. Stucky, *Micro. Meso. Mater.*, 1998, 20, 371-379.
12. D. M. Christie and J. R. Chelikowsky, *J. Phys. Chem. Solids*, 1998, 59, 617-624.
13. Y. C. Liao, S. H. Luo, S. L. Wang, H. M. Kao and K. H. Lii, *J. Solid State Chem,* 2000, 155, 37-41.
14. V. K. Rao, R. Prabhu and S. Natarajan, *Inorg. Chim. Acta*, 2010, 363, 2929-2937.
15. F. M. Tunez, J. Andrade-Gamboa, J. A. Gonzalez and M. R. Esquivel, *Mater. Lett.*, 2012, 79, 202-204.

16. D. Santamaria-Perez, J. Haines, U. Amador, E. Moran and A. Vegas, *Acta Cryst. Sect. B-Struct. Sci.*, 2006, 62, 1019-1024.
17. M. B. Doran, B. E. Cockbain, A. J. Norquist and D. O'Hare, *Dalton. Trans.*, 2004, 3810-3814.
18. T. Berrocal, J. L. Mesa, J. L. Pizarro, L. Lezama, B. Bazán, M. I. Arriortua and T. Rojo, *J. Solid State Chem.*, 2008, 181, 884-894.
19. J. Rouse and M. T. Weller, *Dalt. Trans.*, 2009, 10330-10337.
20. J. A. Armstrong, E. R. Williams and M. T. Weller, *Dalton Trans.*, 2012, 41, 14180-14187.
21. J. A. Armstrong, E. R. Williams and M.T. Weller. *J. Amer. Chem. Soc*. 2011, 133 (21), pp 8252–8263
22. J. A. Armstrong, E. R. Williams and M. T. Weller, *Dalton Trans.*, 2013, 42, 2302-2308.
23. A. C. Keates, J. A. Armstrong and M. T. Weller, *Dalton Trans.*, 2013, 42, 10715-10724.
24. Q. Wang, A. Madsen, J. R. Owen and M. T. Weller, *Chem.l Comm.*, 2013, 49, 2121.
25. J. Axhausen, K. Lux and A. Kornath, *Angew.Chem. Int Ed. Engl.*, 2014, 53, 3720-3721.
26. L. J. Farrugia, *J. Appl. Crystallogr.*, 1999, 32, 837-838.
27. G. Sheldrick, *XPREP. Space Group Determination and Reciprocal Space Plots.*, 1991.
28. G. M. Sheldrick, *Release 97-2*, University of Göttingen, Germany, 1997.
29. G. M. Sheldrick, *Acta Crystallogr. Sect. A: Found. Crystallogr.*, 2008, A64, 112-122.
30. K. L. Marshall and M. T. Weller, *Z. Anorg. Allg. Chem.*, 2014, 640, 2766-2770.
31 A.H.Cowley and R.A.Jones. *Angew. Chem. Int. Ed, Engl.*, 1989, 28, 1208-1215